PROCEEDINGS OF SCIENCE

Measurements of hadron production in pPb collisions in CMS

Krisztián Krajczár[*][†] **on behalf of the CMS Collaboration**
CERN, CH-1211 Geneva 23, Switzerland
E-mail: Krisztian.Krajczar@cern.ch

Spectra of pions, kaons, and protons are measured in pPb collisions at $\sqrt{s_{NN}} = 5.02$ TeV with the CMS detector at the LHC. The particle identification in the laboratory rapidity of $|y_{\mathrm{lab}}| < 1$ and transverse momentum of 0.1–1.7 GeV/c is performed using energies deposited in the silicon tracker. The average transverse momentum is found to increase with particle mass and charged multiplicity of the events. Comparisons to Monte Carlo event generators are performed. The EPOS LHC model, which incorporates additional hydrodynamic evolution of the created system, is able to reproduce most of the data features, unlike HIJING and AMPT. The measured transverse momentum spectra and integrated particle yields are also compared to those observed in pp and PbPb collisions in classes of charged multiplicity at various collision energies. The results indicate that particle production at LHC is strongly correlated with event multiplicity.

The European Physical Society Conference on High Energy Physics -EPS-HEP2013
18-24 July 2013
Stockholm, Sweden

[*]Speaker.
[†]Also at Wigner Research Centre for Physics, 1121 Budapest. Konkoly-Thege Miklós út 29-33, Hungary

PoS(EPS-HEP 2013)181

1. Introduction

The study of hadron spectra is a fundamental part of exploring particle collisions at new centre-of-mass energies. Hadron spectra provide a wealth of constraints and testing opportunities for the implementation of non-perturbative quantum chromodynamics (QCD) processes like hadronization and soft-parton interactions in various Monte Carlo (MC) event generators. Spectra measured in proton-nucleus collisions are also important references for studies of high-energy heavy-ion collisions, where final-state effects are known to modify the spectral shape and yields of different hadron species [1, 2, 3, 4].

2. Detector

A detailed description of the CMS (Compact Muon Solenoid) detector can be found in Ref. [5]. The CMS experiment uses a right-handed coordinate system, with the origin at the nominal interaction point (IP) and the z axis along the counterclockwise-beam direction. The pseudorapidity η and rapidity y of a particle (in the laboratory frame) with energy E, momentum p, and momentum along the z axis p_z are defined as $\eta = \ln[\tan(\theta/2)]$, where θ is the polar angle with respect to the z axis and $y = \frac{1}{2}\ln[(E+p_z)/(E-p_z)]$, respectively. The central feature of the CMS apparatus is a superconducting solenoid of 6 m internal diameter. Within the 3.8 T field volume are the silicon pixel and strip tracker, the crystal electromagnetic calorimeter, and the brass/scintillator hadron calorimeter. The tracker measures charged particles within the pseudorapidity range $|\eta| < 2.4$. It has 1440 silicon pixel and 15148 silicon strip detector modules. In addition to the barrel and endcap detectors, CMS has extensive forward calorimetry. Steel/quartz-fiber forward calorimeters (HF) cover $3 < |\eta| < 5$. Beam Pick-up Timing for the eXperiments (BPTX) devices were used to trigger the detector readout. They are located around the beam pipe at a distance of 175 m from the IP on either side, and are designed to provide precise information on the Large Hadron Collider (LHC) bunch structure and timing of the incoming beams.

3. Experimental methods

A $\sqrt{s_{NN}} = 5.02$ TeV pPb data sample of an integrated luminosity of 1 μb^{-1} (corresponding to a total of 2 M collision events) were used for the measurement of hadron spectra. Due to the asymmetric beam energies the centre-of-mass of the colliding system moves with a rapidity of $y = -0.465$. The particle yields reported in this proceedings have been measured for $|y_{\mathrm{lab}}| < 1$.

Events for analysis were selected by requiring the presence of a track with a transverse momentum (p_T) of at least 0.4 GeV/c reconstructed with the pixel detector in events where both proton and lead beams were present according to BPTX. As part of the offline event selection at least one tower with energy above 3 GeV in each of the HF calorimeters and a reconstruced vertex were required. Beam-halo and beam-induced background events are suppressed following Ref. [6].

The efficiencies for event selection, tracking, and vertexing were evaluated using simulated event samples produced with the HIJING 2.1 MC event generator using the CMS detector simulation framework. Simulated events were reconstructed in the same way as the collision data.

The final results were corrected to a particle level selection applied to the MC output, which is very similar to the data selection described above: at least one particle (proper lifetime $\tau > 10^{-18}$ s) with $E > 3$ GeV in the range $-5 < \eta < -3$ and at least one in the range $3 < \eta < 5$.

The track reconstruction used for the measurement extends to $p_\mathrm{T} \approx 0.1$ GeV/c by exploiting a special tracking algorithm [7, 8]. In order to identify particles at low p_T an analytical parametrization [9] was used to approximate the energy loss in the silicon detectors. The method provides the probability density $P(\Delta|\varepsilon, l)$ of energy deposit Δ, if the most probable energy loss rate ε at a reference path-length l_0 and the actual path-length l are known. It was used in conjunction with a maximum likelihood estimation method. For an accurate determination of ε, the response of all readout chips in the tracker was calibrated with multiplicative gain correction factors. The measured energy deposits were compared to the energy loss parametrization and hit-level corrections were introduced. The best value of ε for each track was calculated with the corrected energy deposits by minimizing the joint energy-deposit negative log-likelihood of all hits on the trajectory. The $\ln\varepsilon$ values in (η, p_T) bins were used to unfold the particle yields. The full description of the procedure can be found in Ref. [8].

4. Results

All the results presented here are from Ref. [10]. In order to extrapolate to $p_\mathrm{T} = 0$ in transverse momentum, and to extract yields dN/dy and average transverse momentum $\langle p_\mathrm{T} \rangle$ a Tsallis-Pareto-type distribution [10, 11] was fitted to the data. The $\langle p_\mathrm{T} \rangle$ and its uncertainty were obtained by numerical integration with the fitted parameters.

The p_T distributions of positive pions, kaons, and protons together with the Tsallis fits can be seen in the left panel of Fig. 1. The right panel shows the measurements in comparison to the predictions of the AMPT 1.26/2.26 [12], EPOS LHC [13, 14], and HIJING 2.1 [15] event generators. EPOS LHC gives a reasonable description of the data, while AMPT and HIJING predict steeper p_T distributions than observed. The distributions for the negative particles are similar [10].

Particle yields are also studied as a function of event multiplicity. This approach is motivated by the observation made in Ref. [8]: in pp collisions the particle production seems to be strongly correlated with event multiplicity rather than with the collision energy. The event multiplicity N_rec is obtained from the number of reconstructed tracks in the $|\eta| < 2.4$ region. The fully corrected charged particle multiplicity N_tracks is also determined for each N_rec event class.

The multiplicity dependence of the ratio of particle yields and the $\langle p_\mathrm{T} \rangle$ is shown in the left and right panel of Fig. 2, respectively. EPOS LHC provides a reasonable description of the data, while the other generators significantly underpredict the measured $\langle p_\mathrm{T} \rangle$.

The comparison of the the particle yields and average transverse momentum to pp [8] and PbPb [16] measurements as a function of event multiplicity can be seen in Fig. 3. The ALICE PbPb data cover a much wider range of N_tracks than is shown in the plot. The horizontal band indicates the diversity of the ALICE results from peripheral to cental collisions. Up to an $N_\mathrm{tracks} \approx 40$ pp and pPb collisions behave very similarly, while at higher multiplicities the $\langle p_\mathrm{T} \rangle$ is lower for pPb than in pp, but both are higher than the ones measured in PbPb. This behaviour can probably be explained by having a different mix of soft and hard collisions at a given N_tracks in the different systems. The ratios of yields are very similar in pp and pPb collisions.

PoS(EPS-HEP 2013)181

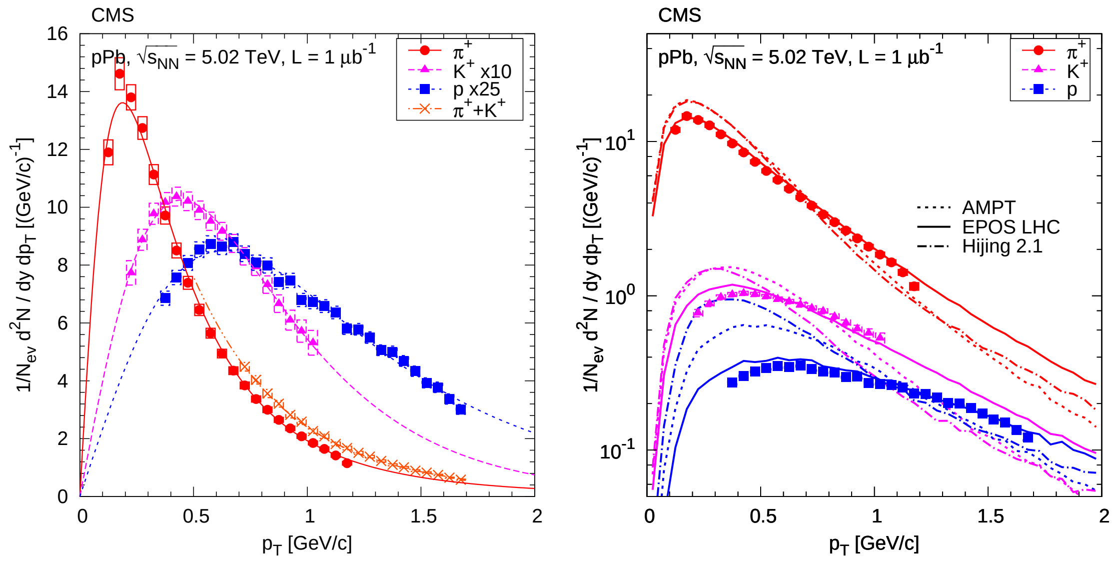

Figure 1: Transverse momentum distributions for positive pions, kaons and protons in the range $|y| < 1$. The left panels shows the Tsallis fits superimposed on data. The right panel presents the comparisons to MC predicitions. Error bars indicate the uncorrelated statistical uncertainties, while boxes show the uncorrelated systematic uncertainties. The fully correlated normalization uncertainty (not shown) is 3.0%

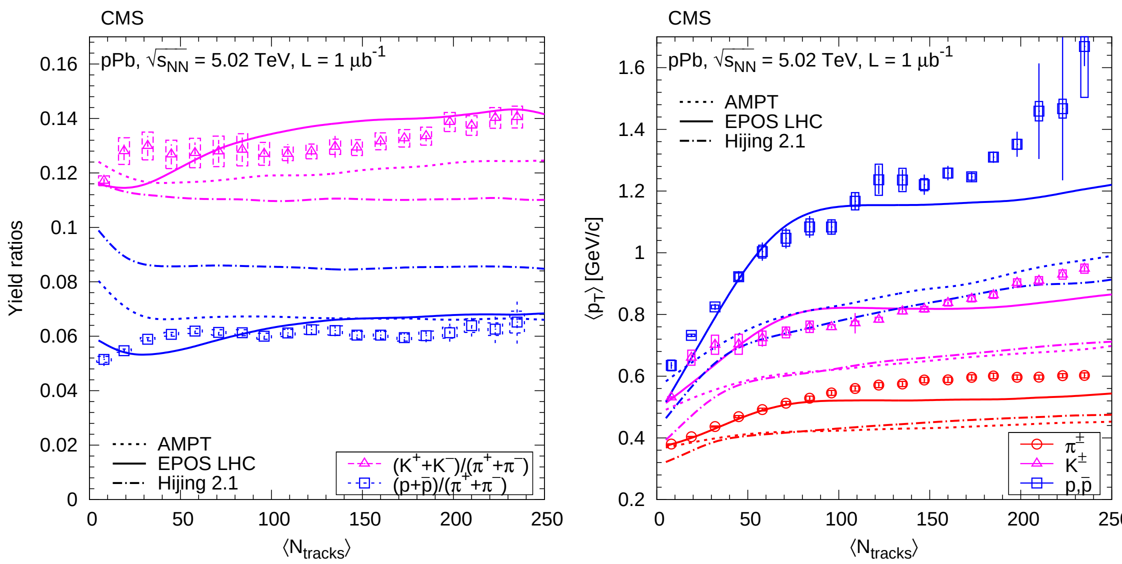

Figure 2: Ratio of particle yields (*left*) and average transverse momentum (*right*) as a function of event multiplicity in $|y| < 1$. Error bars indicate the uncorrelated combined uncertainties, while boxes show the uncorrelated systematic uncertainties.

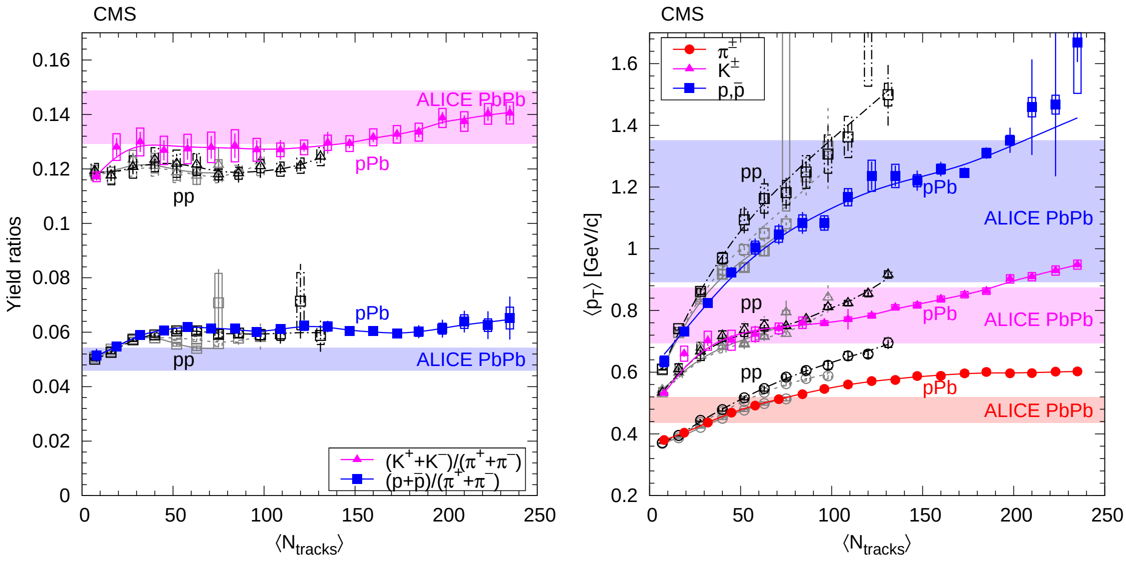

Figure 3: Ratio of particle yields (*left*) and average transverse momentum (*right*) as a function of event multiplicity measured in pPb collisions shown in comparison to pp [8] and PbPb [16] data. Error bars indicate the uncorrelated combined uncertainties, while boxes show the uncorrelated systematic uncertainties. Lines are drawn to guide the eyes.

Motivated by the success of Boltzmann-type distributions in nucleus-nucleus collisions the p_T distributions were also fitted with a function proportional to $p_T \exp(-m_T/T')$, were T' is the inverse slope parameter. This inverse slope parameter as a function of the hadron mass for various multiplicity bins is presented in Fig. 4. The left panel shows the measured values, while the right panel presents the MC expectations. The linear dependence displayed by data is not reproduced by the MC models. The models predict a flat or slowly rising behavior as a function of mass and only limited changes with track multiplicity. In case of nucleus-nucleus collisions the linear trend is attributed to the effect of radial flow velocity boost [1]. However, interestingly both pp data and pp MC generators [8] show features very similar to those observed in the pPb data.

Acknowledgments The author wishes to thank the Hungarian Scientific Research Fund (NK-81447, K-81614) for its support.

References

[1] E. Schnedermann, J. Sollfrank, and U. W. Heinz, *Thermal phenomenology of hadrons from 200 AGeV S+S collisions*, *Phys. Rev. C* **48** (1993) 2462 [`arXiv:nucl-th/9307020`].

[2] PHENIX Collaboration, *Identified charged particle spectra and yields in Au+Au collisions at* $\sqrt{s_{NN}} = 200$ *GeV*, *Phys. Rev. C* **69** (2004) 034909 [`arXiv:nucl-ex/0307022`].

[3] PHOBOS Collaboration, *Identified hadron transverse momentum spectra in Au+Au collisions at* $\sqrt{s_{NN}} = 62.4$ *GeV*, *Phys. Rev. C* **75** (2007) 024910 [`arXiv:nucl-ex/0610001`].

[4] STAR Collaboration, *Systematic Measurements of Identified Particle Spectra in pp, d+Au and Au+Au Collisions from STAR*, *Phys. Rev. C* **79** (2009) 034909 [`arXiv:0808.2041`].

[5] CMS Collaboration, *The CMS experiment at the CERN LHC*, *JINST* **3** (2008) S08004.

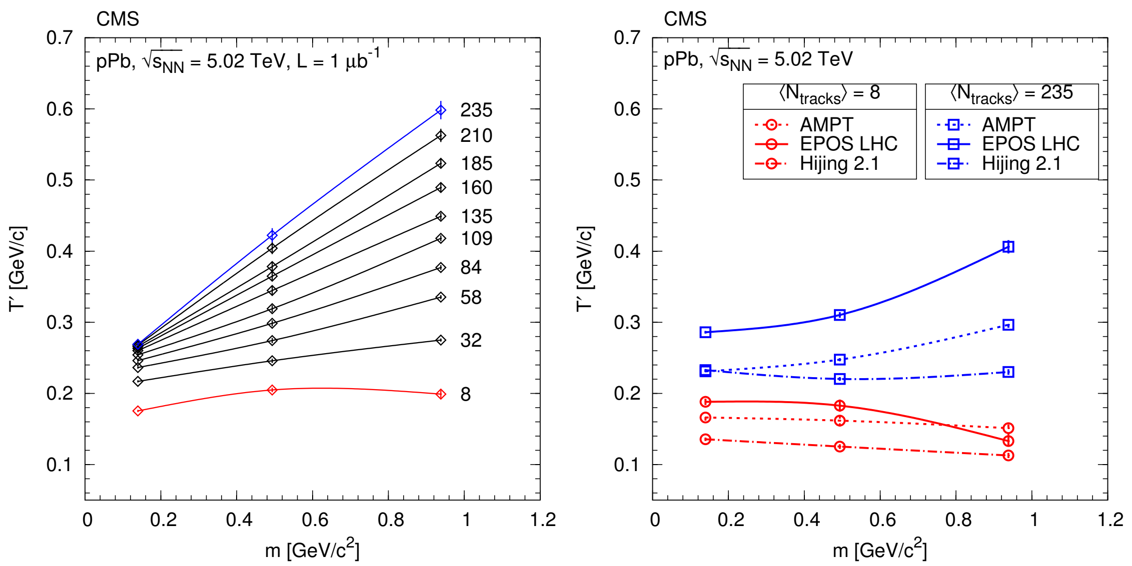

Figure 4: Inverse slope parameter obtained from $p_T \exp(-m_T/T')$ fits to the transverse momentum distributions for pions, kaons and protons for various multiplicity classes. The left panel shows the measured valies, while the right panel presents MC predictions. The curves are drawn to guide the eye.

[6] CMS Collaboration, *Transverse momentum and pseudorapidity distributions of charged hadrons in pp collisions at $\sqrt{s} = 0.9$ and 2.36 TeV*, *JHEP* **02** (2010) 041 [`arXiv:1002.0621`].

[7] F. Siklér, *Low p_T Hadronic Physics with CMS*, *Int. J. Mod. Phys. E* **16** (2007) 1819 [`arXiv:physics/0702193`].

[8] CMS Collaboration, *Study of the inclusive production of charged pions, kaons, and protons in pp collisions at $\sqrt{s} = 0.9$, 2.76, and 7 TeV*, *Eur. Phys. J. C* **72** (2012) 2164 [`arXiv:1207.4724`].

[9] F. Siklér, *A parametrisation of the energy loss distributions of charged particles and its applications for silicon detectors*, *Nucl. Intrum. Meth. A* **691** (2012) 16 [`arXiv:1111.3213`].

[10] CMS Collaboration, *Study of the production of charged pions, kaons, and protons in pPb collisions at $\sqrt{s_{NN}} = 5.02$ TeV*, (2013) [`arXiv:1307.3442`].

[11] C. Tsallis, *Possible generalization of Boltzmann-Gibbs statistics*, *J. Stat. Phys.* **52** (1988) 479.

[12] Z. W. Lin, *Current status and further improvements of a multi-phase transport (AMPT) mode*, *Indian J. Phys.* **85** (2011) 837.

[13] K. Werner, F.-M. Liu, and T. Pierog, *Parton ladder splitting and the rapidity dependence of transverse momentum spectra in deuteron-gold collisions at RHIC*, *Phys. Rev. C* **74** (2006) 837 [`arXiv:hep-ph/0506232`].

[14] T. Pierog et al, *EPOS LHC : test of collective hadronization with LHC data*, (2013) [`arXiv:1306.0121`].

[15] W.-T. Deng, X.-N. Wang, and R. Xu, *Hadron production in p+p, p+Pb, and Pb+Pb collisions with the HIJING 2.0 model at energies available at the CERN Large Hadron Collider*, *Phys. Rev. C* **83** (2011) 014915 [`arXiv:1306.0121`].

[16] ALICE Collaboration, *Centrality dependence of π, K, p production in Pb-Pb collisions at $\sqrt{s_{NN}} = 2.76$ TeV*, (2013) [`arXiv:1303.0737`].